Particle Size Improvement by a Countercurrent Tower Crystallizer

A continuous, staged-feed column crystallizer was investigated to obtain enlarged product size distribution in precipitation from solution. Stage population balances, in moment form, were solved analytically for several single-feed configurations. It was found that internal staging permits control of the solids concentration profile, and if collision nucleation is unimportant then countercurrent operation yields the greatest product size enlargement. Nucleation kinetic parameters for a given salt indicate the potential product size improvement, compared to product from an MSMPR crystallizer of equal volume.

R. W. Farmer and J. R. Beckman
Chemical and Bio Engineering Department
Arizona State University
Tempe, AZ 85287

SCOPE

In crystallization processes the concept of staging typically appears in the form of cascades of separate stirred-tank crystallizers. Generally, such arrangements permit closer control of product crystal size distribution (CSD) than does a large single crystallizer of identical total volume (Larson and Wolff, 1971). A more economical approach may be to incorporate these individual crystallizers into a single unit while retaining the benefits of staging. This is the motivation for the current investigation of a staged-feed column crystallizer for enlargement of product CSD.

Previous studies involving column crystallizers have dealt exclusively with improving the purity of crystals produced from melts (Betts and Girling, 1971; Mullin, 1980; Matz, 1980; Takegami et al., 1984). Mathematical development of simulation models for countercurrent column melt crystallizers has been presented by Player (1969), and more recently by Chien (1984). However, these examples do not deal directly with product CSD. For crystallization from solution, product CSD is recognized as the primary indicator of performance.

The configuration of the multistage crystallizer is essentially a mixed column, which may be divided by internal baffles into a number of cylindrical stages. Interstage backmixing transports product solids both down the tower, and upward following the predominant bulk upflow. A conical clarifier connected to the uppermost stage returns solids to the column and delivers an essentially solids-free overflow stream. Feed streams, usually aqueous salt solutions, may be distributed to the stages, permitting control of solids production rate in each stage.

A mathematical model has been developed to describe the multistage column crystallizer. Population balances for all stages were written, then reduced to multiple sets of algebraic equations using the method of moments (Randolph and Larson, 1962, 1971; Randolph and Tan, 1978; Beckman and Farmer, 1984). A three-parameter power law form was employed to model nucleation rate, so that the equations for the four leading moments, along with a solute balance, constitute a closed set.

Applying this model, the performance of the staged crystallizer was simulated for units having single feed and product streams. More generally, the staged-feeding feature permits any distributed feed profile; however, for the single-feed case an explicit analytical solution is obtained. Calculated results illustrate the importance of feed/product location, interstage backmixing rate, and nucleation kinetic parameters, with respect to product size enlargement. In all cases, the

Correspondence concerning this paper should be addressed to J. R. Beckman.

volume-averaged mean product size from the staged crystallizer is compared to that from a single-stage unit (MSMPR) for identical operating conditions and total crystallizer volume.

An experimental example is also described for gypsum ($CaSO_4 \cdot 2H_2O$) production from sodium sulfate (Na_2SO_4) and calcium chloride ($CaCl_2$) feeds. A comparison of mean product sizes obtained from four-stage and single-stage crystallizer runs was interpreted on the basis of nucleation kinetic criteria.

CONCLUSIONS AND SIGNIFICANCE

There are a large number of pertinent design and operating variables associated with the countercurrent staged-feed (CCSF) crystallizer. A few of these variables have been manipulated, and their importance examined, using a population balance model. The variables considered were the number of stages, interstage backmixing rate, the location of single feed and product streams, and the values of the nucleation kinetic exponents for a power law model.

The key to product size enlargement in the staged crystallizer is the relative responses of growth and nucleation rates to variation in solids concentrations. Depending on the number of stages and the arrangement of feed and product streams, the solids concentration within the growth stage (i.e., that which receives *feed*) may be greater than, equal to, or less than that in a mixed-suspension, mixed-product-removal (MSMPR) crystallizer having equal total volume. For a given solids production rate, the resultant decrease in growth rate at high suspension densities will suppress primary (e.g., homogeneous) nucleation. However, the power law nucleation model also includes the effect of secondary mechanisms that tend to increase the net nucleation rate as suspension density increases. It has been shown that the relative strength of primary vs. secondary nuclei sources, as indicated by the values of kinetic model parameters, is the most important criterion in predicting product size enlargement.

A pure countercurrent feed/product arrangement yields the most marked amplification of solids concentration. Therefore, it is to be favored if secondary nuclei sources are weaker than primary nucleation. Experimental comparison of gypsum product CSD from a four-stage CCSF crystallizer with that from a single-stage unit reveals only modest size enlargement, since both nuclei sources are of comparable strength. Analytical results show that for such applications enlarged product may still be obtained by using fewer stages and rearranging the feed/product stream locations.

The effect of increasing the number of stages also depends on the influence of secondary nucleation. Should primary nuclei sources predominate, product size always increases as the number of stages increases. In general, high backmixing rates have been shown to reduce product size. This is because the stage suspension densities more closely approach that of a single uniform stage, negating the benefit of internal staging.

The CCSF crystallizer represents a new unit operation for many crystallization applications. A *profile in* stage solids concentrations is induced by mixed column hydrodynamics; combined with flexibility in solute feed location, this allows the crystal growth rate and solute feed rate to be independently controlled. This concept offers the potential for CSD enlargement, thus reducing downstream dewatering and filtration costs, while increasing product value.

Introduction

A number of ideas have been proposed to obtain enlarged product crystal size distribution (CSD) from MSMPR-type crystallizers. Cascades of simple MSMPR crystallizers offer improved control over product CSD (Larson and Wolff, 1971), but at greater capital cost, due to duplication of mixers, slurry pumps, and other hardware. Conceptually, a multistage column crystallizer offers product size enlargement and the control advantages of staging without redundancy of equipment.

The concept of a staged column crystallizer for production of sparingly soluble precipitates was first introduced by Beckman and Farmer (1984). Countercurrent tower crystallizers have been employed in many applications to improve the purity of crystals produced from melts. Numerous examples have been described in the literature (Henry and Powers, 1970; Betts and Girling, 1971; Devyatykh et al., 1977; Matz, 1980; Takegami et al., 1984; Mullin, 1980). Player (1969), and more recently Chien (1984), have presented the mathematical development for simulation of a continuous, countercurrent crystallizer in the purification of melts. None of these examples deals with product CSD. Crystallization of precipitates is currently carried out in MSMPR-type crystallizers, for which product CSD is the primary concern.

In this paper a general mathematical model simulating the countercurrent staged feed crystallizer is developed. Product size enlargement is shown to be highly dependent on column feed/product stream arrangement, interstage backmixing rate, and nucleation kinetics. As an example, data for a crystallizer producing gypsum ($CaSO_4 \cdot 2H_2O$) from aqueous Na_2SO_4 and $CaCl_2$ feeds are presented.

Process Description

A countercurrent staged-feed (CCSF) crystallizer, as shown in Figure 1, may be envisioned as a number of individual crystallizer stages superimposed on mixed column hydrodynamics. A solution containing soluble salt anion (stream 1) is fed predomi-

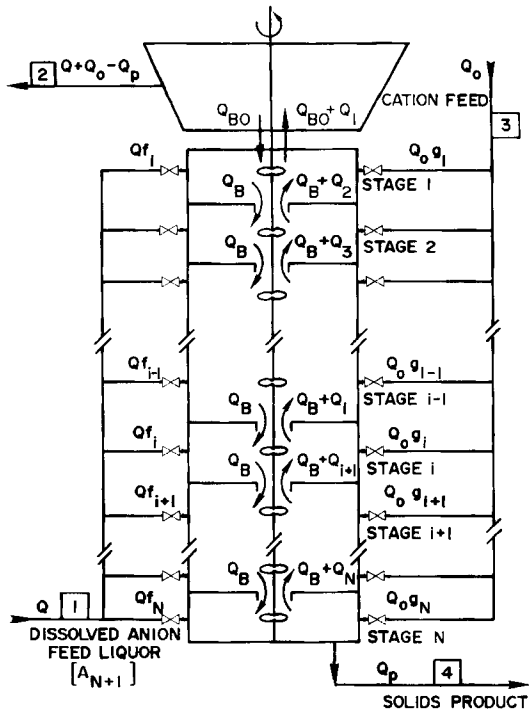

Figure 1. Countercurrent staged-feed (CCSF) crystallizer.

nantly to the lower stages, and provides bulk upflow. The complementary cation is fed in either solution or slurry form (stream 3). Theoretically, the feeds may be introduced to the stages in any desired profile, permitting control of the stage residence times and magma concentrations. One or more streams containing product solids are withdrawn from any stage in the column (e.g., stream 4).

Backmixing streams flow via center ports in the stator plates separating adjacent stages. Product solids are transported by interstage backmixing both down the tower, and upward following the upflow liquor. Material entering each stage in this manner provides a source of crystal surface area, simultaneously reducing the rates of crystal growth and primary nucleation. Staged crystallizer hydrodynamics induce a profile in solids concentration, resulting in total solids holdup greater than that in an MSMPR crystallizer of equivalent volume. This effect is then amplified as the number of stages increases. Physically, suppressed nucleation due to increased solids holdup explains why the staged crystallizer delivers larger size product than an MSMPR unit. This benefit is negated, however, if collision breeding dominates primary nucleation.

The CCSF crystallizer is currently operated isothermally, so that temperature effects on product solubility are unimportant. This does not rule out the possibility of operation as a cooling crystallizer, to improve yield, or as a reactor crystallizer [e.g., HSO_3^-(aq) and $Ca(OH)_2$(s) feeds giving $CaSO_3 \cdot \frac{1}{2} H_2O$ product]. The first-generation CCSF crystallizer examined here does not include fines destruction or product classification. These techniques are widely applied industrially for product size enhancement, especially when supersaturation is brought about by a temperature differential. Conceivably these features could be incorporated into a multistage column crystallizer, but at the expense of much greater geometric complexity.

Several important operating assumptions are made in the analysis presented here. First, no interstage classification is permitted; that is, the complete CSD existing in a given stage is carried by the streams leaving that stage. Consequently, *perfect* mixing must be imposed within each stage. Analysis is greatly simplified if the CCSF crystallizer is operated in class II mode, meaning complete intrastage consumption. This requires that all of the limiting ion fed to any stage be converted to product solid phase within that stage. It is possible that some solids concentration effects, due to sedimentation or particle entrainment, may occur at the stator ports and/or the product port without resulting in classification. Such effects are included in the mathematical modeling.

Any solids entrained in the overflow liquor would reduce the net product yield. To minimize this, a clarifier is connected to the top stage of the column crystallizer. This unmixed chamber permits settled product solids to be reintroduced to the active crystallizer volume via interchange flow with the clarifier. The solids-free clarifier overflow thus corresponds to the clear-liquor-advance feature common in conventional crystallizer systems.

In this paper, crystallizer configurations having single cation feed and product streams are considered. For simplicity the anion solution feed is introduced to the bottom CCSF crystallizer stage in all cases. As a basis for comparisons the ratio $\bar{L}_N/\bar{L}_{MSMPR}$ is used, where $\bar{L}$ $(=m_3/m_2)$ is the volume averaged particle size of the product, and the MSMPR subscript refers to the single-stage base case having identical active volume and feed rates as the N-stage unit. For the single-feed case, if secondary nucleation effects are minor, it is shown that largest size product is obtained when feeds are introduced in a "pure countercurrent" fashion. This refers to single cation feed to the top stage, with product withdrawn from the bottom stage of the column.

Theoretical Development

Population balances may be written describing each CCSF crystallizer stage by the method of Randolph and Larson (1962, 1971). Referring to Figure 2, these are of the following form for the general case of feed streams to each stage:

$$y_i n_{i-1}(L) - n_i(L) + x_i n_{i+1}(L) = -\tau_i G_i \frac{dn_i}{dL} \qquad (1)$$

Dimensionless coefficients x_i and y_i are composed of bulk upflow and backmixing flowrates Q_i and Q_B, respectively, as shown in Table 1. The population density function, $n(L)$, is defined as the number of particles having a characteristic dimension L (equivalent spherical diameter) within differential size interval, dL. In the balance for stage i the n_{i-1} term represents solids transport from the adjacent upward stage, and similarly the n_{i+1} term is associated with solids inflow from the adjacent lower stage. The righthand side of Eq. 1 is the crystal growth term, with the definition of stage residence time τ_i based on total liquid outage from stage i. Appropriate specific forms of Eq. 1 for each CCSF crystallizer stage are given in Table 1.

Note the appearance of parameter θ, associated with the Q_B terms in the definitions of x_i and y_i. Depending on its sign, this parameter either augments or diminishes the effective solids transport by backmixing, thus accounting for interstage mass concentration effects mentioned previously. Parameter P has an analogous role for the product stream withdrawal port.

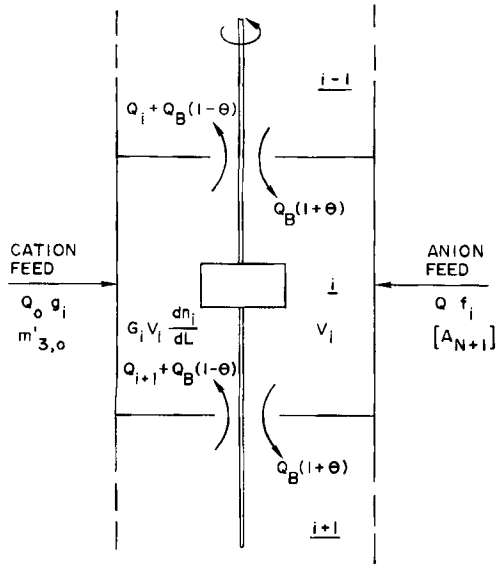

Figure 2. Terms contributing to CCSF crystallizer internal stage population balance.

For $i = 0$, only fines smaller than some critical size L_C are assumed to be present in the overflow stream. Coefficient S is a unit step function that equals unity for $0 < L < L_C$. For a given upflow rate, L_C depends on clarifier design and must be verified experimentally; the clarifier unit used here was designed for $L_C = 10\ \mu$m, based on laminar (Stokes law) sedimentation.

It is necessary to impose a kinetic statement for nucleation. A commonly applied nucleation model is:

$$B^o = \kappa_n G^g m_3^j = n^o G \tag{2}$$

This form has been employed by Randolph and Larson (1971), Younquist and Randolph (1972), Desai et al. (1974), and others, to incorporate secondary nucleation effects. White and Hoa (1977), and Etherton and Randolph (1981), have used this model for gypsum nucleation.

Solving the set of ordinary differential equations given in Table 1 is impractical since the growth rates, G_i, are not known a priori. By the method of moments (Randolph and Tan, 1978) these may be reduced to four sets of algebraic equations corresponding to the four leading moments of the CSD. Multiplying Eqs. T1 through T3 from Table 1 by $L^k dL$ and integrating over $0 < L < \infty$, gives (e.g., for $1 < i < N$):

$$k = 0; \quad y_i m_{0,i-1} - m_{0,i} + x_i m_{0,i+1} = -G_1 \tau_i n_i^o \tag{3}$$

$$k = 1, 2, 3; \quad y_i m_{k,i-1} - m_{k,i} + x_i m_{k,i+1} = -k\tau_i G_i m_{k-1,i} \tag{4}$$

where the definition of the kth order moment has been substituted:

$$m_k = \int_o^\infty n(L) L^k dL \tag{5}$$

and Eq. T0 was used to eliminate n_o from Eq. T1.

Substitution of the kinetic model for the nuclei density parameter, n^o, yields the final forms summarized in Table 2. In the $i = 1$ equations the Γ terms are fractional moments representing material washed out via the overflow stream:

$$\Gamma_k = z_1 \int_o^{L_c} n_1(L) L^k dL. \tag{6}$$

These sets of equations are more readily manipulated in matrix form;

$$\begin{bmatrix} m_{0,1} \\ \cdot \\ \cdot \\ \cdot \\ m_{0,N} \end{bmatrix} = -\kappa_n B^{-1} \cdot \begin{bmatrix} G_1^g & \tau_1 & m_{3,1}^j - \Gamma_o \\ & & \cdot \\ & & \cdot \\ & & \cdot \\ G_N^g & \tau_N & m_{3,N}^j \end{bmatrix} \quad \text{for } k = 0 \tag{7}$$

$$\begin{bmatrix} m_{k,1} \\ \cdot \\ \cdot \\ \cdot \\ m_{k,N} \end{bmatrix} = -kB^{-1} \cdot \begin{bmatrix} G_1 & \tau_1 & m_{k-1,1} - \Gamma_1 \\ & & \cdot \\ & & \cdot \\ & & \cdot \\ G_N & \tau_N & m_{k-1,N} \end{bmatrix} \quad \text{for } k = 1, 2, 3 \tag{8}$$

Matrix B is the tridiagonal coefficient matrix; it is identical for all k, and consists of dimensionless coefficients x, y, and z, as shown in Table 3.

A solute balance on the product solid phase, based on complete intrastage consumption, may be written for each stage:

$$\tfrac{1}{2} G_i \tau_i \rho_s \gamma m_{2,i} = f_i([A_{N+1}] - [A]_i) \quad 1 \le i \le N$$

for anion species limiting

$$= g_i \rho_s' m_{3,0}' Q_o \quad 1 \le i \le N \tag{9}$$

for cation species limiting (slurry form)

Table 1. CCSF Crystallizer Stage Population Balances

$i = 0; n_0 = S n_1$ (T0)

$i = 1; z_1 n_0 - n_1 + x_1 n_2 = G_1 \tau_1 \dfrac{dn_1}{dL}$ (T1)

$$z_1 = \frac{Q_{B0}}{Q_1 + Q_{B0} + Q_B(1+\theta)}; \quad x_1 = \frac{Q_2 + Q_B}{Q_1 + Q_{B0} + Q_B(1+\theta)}$$

$$\tau_1 = \frac{V_1}{Q_1 + Q_{B0} + Q_B(1+\theta)}$$

$2 \le i \le N-1; \quad y_i n_{i-1} - n_i + x_i n_{i+1} = G_i \tau_i \dfrac{dn_i}{dL}$ (T2)

$$y_i = \frac{Q_B(1+\theta)}{Q_i + 2Q_B}; \quad x_i = \frac{Q_{i+1} + Q_B(1-\theta)}{Q_i + 2Q_B}; \quad \tau_i = \frac{V_i}{Q_i + 2Q_B}$$

$i = N; \quad y_N n_{N-1} - n_N = G_N \tau_N \dfrac{dn_N}{dL}$ (T3)

$$y_N = \frac{Q_B(1+\theta)}{Q_l + Q_B(1-\theta) + P Q_p}; \quad \tau_N = \frac{V_N}{Q_N + Q_B(1-\theta) + P Q_p}$$

Table 2. Moment-Transformed Population Balances

$i = 1$;	$k = 0$	$-z_1 m_{0,1} + m_{0,2} = -\tau_1 \kappa_n G_1^{\ell} m_{3,1}^{j} - \Gamma_0$	(T4)
	$k = 1,2,3$	$-z_1 m_{k,1} + x_1 m_{k,2} = -k\,\tau_1 G_1\, m_{k-1,1} - \Gamma_k$	(T5)
		$\Gamma_k = z_1 \int_0^{L_c} n_1(L)\, L^k dL\; k = 0,1,2,3$	(T6)
$2 \le i \le N-1$;	$k = 0$	$y_i m_{0,i-1} - m_{0,i} + x_i m_{0,i+1} = -\tau_i \kappa_n G_1^{\ell} m_{3,i}^{j}$	(T7)
	$k = 1,2,3$	$y_i m_{k,i-1} - m_{k,i} + x_i m_{k,i+1} = -k\,\tau_i G_i\, m_{k-1,i}$	(T8)
$i = N$;	$k = 0$	$y_N m_{0,N-1} - m_{0,N} = -\tau_N \kappa_n G_N^{\ell} m_{3,N}^{j}$	(T9)
	$k = 1,2,3$	$y_N m_{k,N-1} - m_{k,N} = -k\,\tau_N G_N\, m_{k-1,N}$	(T10)

When these are included with the set of N moment equations closure is achieved for the five unknowns: growth rate G_i, and four moments $m_{k,i}$.

Presuming cation species limiting, it can be seen from Eq. 9 that if feed fraction g_i is zero to any stage then the growth rate within that stage must also be zero. In the case of a single cation feed stream only one number of the righthand side vector in Eqs. 7 and 8 is nonzero. This simplification permits an explicit analytical solution to be obtained. The third moments, $m_{3,i}$, are calculable independently from cation species material balances. After substitution for $m_{3,i}$, the resulting form of Eq. 7 may be solved for the zeroth moments in terms of the single nonzero growth rate. In Eq. 8 the $k-1$ order moment appears on the righthand side of the kth-order moment equation. This allows a sequential matrix inversion procedure in solving for the remaining moments for all stages in terms of the third moments and unknown growth rate. Finally, solving Eq. 8, with $k = 3$, and Eq. 9 simultaneously yields a value for the growth rate.

Table 3. Recursion Form of Flow Factor as Derived from Coefficient Matrix, *B*

No. of Stages, N	β_N (Pure Countercurrent)
2	$z_1 - x_1 y_2$
3	$z_1 - \dfrac{x_1 y_2}{1 - x_2 y_3}$
4	$z_1 - \dfrac{x_1 y_2}{1 - \dfrac{x_2 y_3}{1 - x_3 y_4}}$
5	$z_1 - \dfrac{x_1 y_2}{1 - \dfrac{x_2 y_3}{1 - \dfrac{x_3 y_4}{1 - x_4 y_5}}}$

Tridiagonal Coefficient Matrix for Moment Balances

$$\mathbf{B} = \begin{bmatrix} -z_1 & x_1 & 0 & \cdot & \cdot & \cdot & 0 \\ y_2 & -1 & x_2 & 0 & \cdot & \cdot & 0 \\ 0 & y_3 & -1 & x_3 & 0 & \cdot & \cdot \\ 0 & 0 & y_4 & -1 & x_4 & \cdot & \cdot \\ \vdots & & & & \cdot & \cdot & \vdots \\ 0 & 0 & \cdot & \cdot & 0 & y_N & -1 \end{bmatrix}$$

A useful design equation for evaluating CCSF crystallizer performance for the single-feed case can be derived from:

$$\frac{\bar{L}_N}{\bar{L}_{\text{MSMPR}}} = \frac{(m_3/m_2)_N}{(m_3/m_2)_{\text{MSMPR}}} \tag{10}$$

When the moment expressions derived following the above procedure for N-stage and single-stage crystallizers are substituted into Eq. 10, the final form is, after some rearrangement:

$$\frac{\bar{L}_N}{\bar{L}_{\text{MSMPR}}} = N^{1-\ell/\ell+3} \left(\frac{\beta_N Q_1 + 2Q_B}{PQ_p} \right)^{j-\ell/\ell+3} \tag{11}$$

Equation 11 is valid for equal volume stages ($V_i = V_T/N$), backmixing streams Q_B and Q_{Bo} equal, and assuming $L_c = 0$. Flow factor β_N is a dimensionless parameter characteristic of the number of tower stages and flow rates Q_i and Q_B. The recursion forms for β_N given in Table 3 arise from the inversion of matrix B in solving Eqs. 7 and 8 for the pure countercurrent, top-stage feed configuration. Other feed locations give slightly different forms for β_N, as will be shown by an example. While the design equation does include the empirical parameter θ, the following analysis assumes θ to be essentially zero. Equation 11 is independent of crystallizer volume because both the MSMPR base case and N-stage CCSF crystallizers are assumed to have identical volumes.

Analytical Results

Using Eq. 11, the importance of several factors may be examined with respect to simulated CCSF crystallizer performance. Figure 3 shows the effect of increasing the number of stages for three combinations of kinetic exponents. The presumed operating conditions for a pure countercurrent arrangement, having cation fed only to the top stage, are also given. As might be expected, the product size improvement increases with the number of stages. However, this trend sharply declines when secondary (i.e., collision) nucleation becomes significant, as reflected by kinetic exponent j being nonzero.

The impact of secondary mechanisms is also evident in Figure 4. Carrying along the same set of operating conditions for a three-stage crystallizer with $\ell = 1$ and $j = 0$, it is seen that product size enlargement of a factor of five or more is possible at low levels of backmixing. This benefit is generally diminished if exponent j is increased to 1.0. The decrease in $\bar{L}_3/\bar{L}_{\text{MSMPR}}$ as Q_B increases is reasonable, since the solids concentrations within the multistage tower more closely approach that in a single-stage unit as backmixing becomes more intense.

The three-stage simulation may be extended to include illustrative examples of other feed and product withdrawal arrangements. For middle-stage feed location the form of the flow factor coefficient is as follows:

$$\beta_{3m} = 1 - y_3 x_2 - \frac{y_2 x_1}{z_1} \tag{12}$$

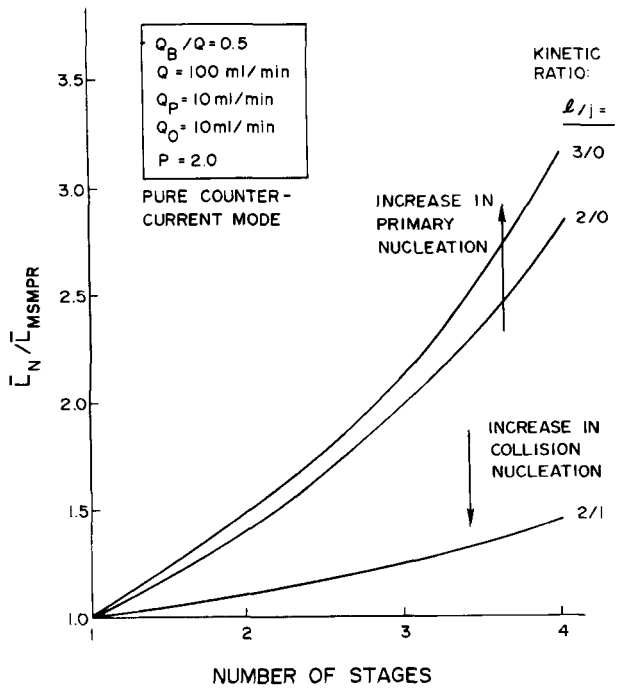

Figure 3. Predicted mean product size ratio vs. number of stages: relative importance of nucleation mechanisms.

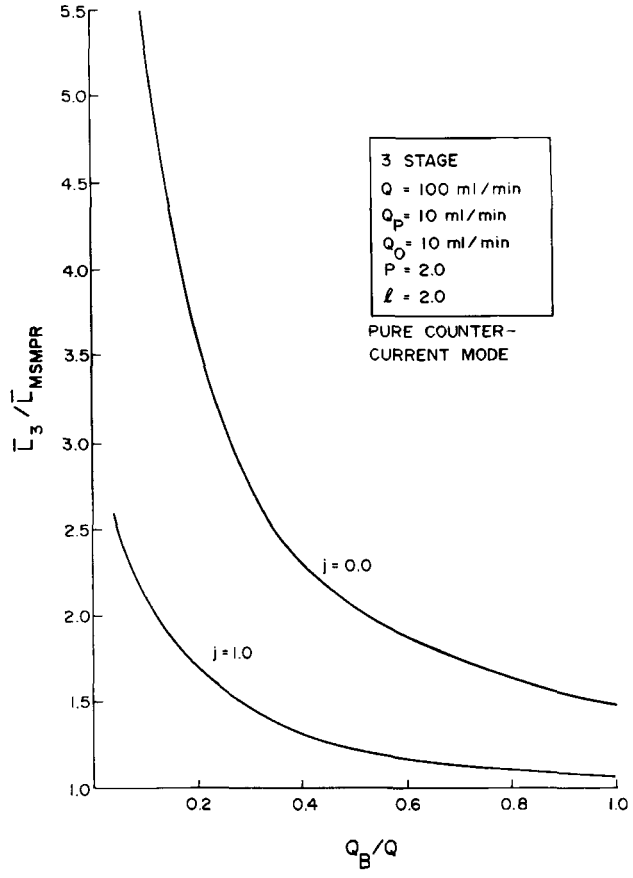

Figure 4. Predicted mean product size ratio for a three-stage CCSF crystallizer vs. backmixing ratio, including the influence of significant (j = 1.0) and negligible (j = 0.0) secondary nucleation.

Again, β_{3m} is derived from the solution of the appropriate matrix form of Eqs. 7 and 8.

If the feed is moved to the lower stage it can be shown that the size improvement ratio is independent of j:

$$\left(\frac{\bar{L}_N}{L_{MSMPR}}\right)_b = \left(\frac{N\beta_{Nb}(Q_N + Q_B + PQ_p)}{PQ_p}\right)^{1-\ell/\ell+3} \tag{13}$$

where for $N = 3$:

$$\beta_{3b} = \frac{z_1 - y_2x_1}{y_2x_1 - z_1(y_3x_2 - 1)} \tag{14}$$

From material balances it is apparent that the solids concentration in the product stream of an N-stage crystallizer must match that in the corresponding single stage MSMPR. Therefore, the ratio $m^j_{3,p}/m^j_{3,MSMPR}$, which arises in the derivation of Eq. 11, equals unity for any value of j.

Continuing with the previous three-stage example, simulated results for several feed/product configurations are shown in Figure 5 and 6. If secondary nucleation is unimportant, that is, j = 0, then the pure countercurrent arrangement yields the greatest benefit for virtually all positive values of exponent ℓ. Similar calculations for $j = 1$, as depicted in Figure 6, indicate that the pure countercurrent mode delivers product size improvement only for $\ell > 1$. For smaller values of exponent ℓ, feed to either the top or bottom stages, with product removed from the same stage, yields greater size improvement. For all cases, the magnitude of product size enlargement declines for $j > 0$. This again points out the importance of secondary nucleation as a limitation of CCSF crystallizer performance.

The trends depicted in Figures 5 and 6 can be physically interpreted with reference to Figure 7. This shows the solids concentration profiles as calculated from limiting species material balances for each of the five example column arrangements. These profiles, normalized to the solids concentration in a homogeneous MSMPR crystallizer, illustrate the flexibility of a staged column with respect to control of solids holdup.

In particular, it is important to recognize the connection between the stage solids concentrations and product size obtained. Depending on the response of total nucleation rate to variation in crystal surface area, it may be favorable to introduce feed to a stage containing higher or lower concentration than the equivalent MSMPR unit. What the staged crystallizer allows is independent control of feed rate and crystal growth rate to an extent not feasible in uniformly-mixed crystallizers. This enhanced level of control can be exploited in a variety of applications for which high nucleation rates may limit product size.

In evaluating the CCSF crystallizer for any particular application a chart such as Figure 8 is useful. Each line represents a break-even boundary, obtained by setting $\bar{L}_N/\bar{L}_{MSMPR} = 1.0$ in Eq. 11. The half-plane below each line is the kinetic regime for which the CCSF crystallizer yields product size improvement, based on the operating conditions shown. Of interest is that for $j > 1.0$, $\ell > 1.0$, size improvement becomes greater with fewer stages. This is because as the number of stages increases, so does the total solids holdup in the crystallizer. Consequently, for $j >$

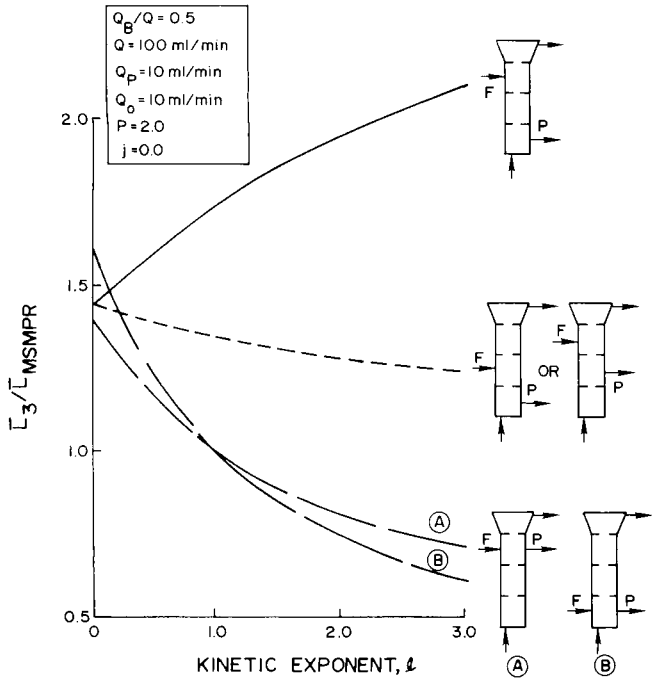

Figure 5. Shift in product size trends vs. primary nucleation exponent, ℓ, as predicted for feed and product stream configurations, negligible secondary nucleation (j = 0.0).

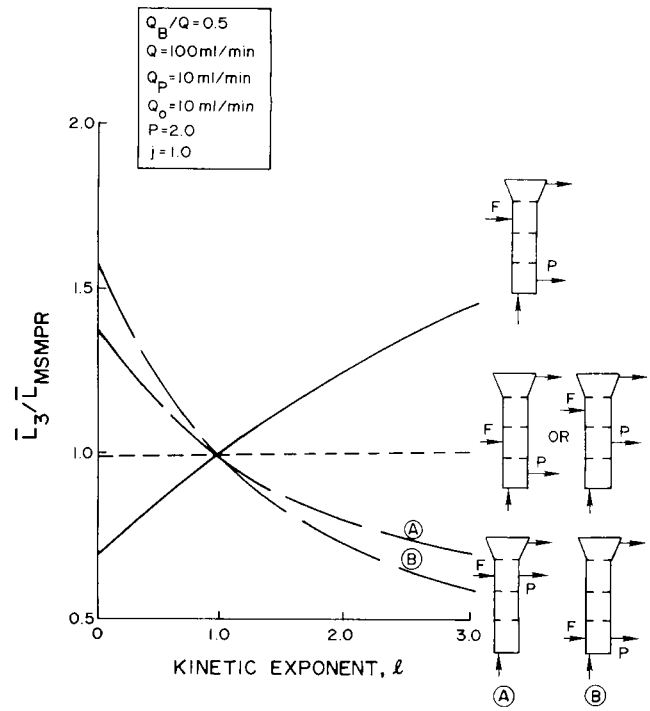

Figure 6. Shift in product size trends vs. primary nucleation exponent, ℓ, as predicted for feed and product stream configurations, including secondary nucleation effect (j = 1.0).

1.0 secondary nucleation effects increase, reducing product size.

Another observation with regard to Figure 8 concerns point A, which represents the kinetic exponent values obtained during the course of this work for gypsum nucleation. Based on these kinetics, only a slight product size improvement is to be expected for gypsum. This result was verified experimentally as shown by the sample data to follow.

Experimental

A lab-scale CCSF crystallizer was constructed having 2.5 L active volume. The tower was 10.2 cm ID and the total height of the active region was adjustable so as to keep total active volume constant for any number of stages. Peristaltic pumps were employed for feed delivery and product withdrawal. Connected to the top stage of the column was a conical glass clarifier; the top diameter of 15.2 cm was sized to allow for settling of particles larger than 10 μm equivalent diameter at the flow rates used. Material used for the column was clear acrylic plastic.

Given the importance of secondary nucleation as an inhibitor of CCSF crystallizer performance, the internals design sought to maximize mixedness at low impeller speed. Based on the work of Zwietering (1958), two-blade paddle impellers were chosen since this type delivers greater circulating flow with less impeller surface, and at low impeller speed. Four 1.0 cm vertical baffles were attached to the column walls to improve mixing.

A separate column apparatus having identical geometry was used to experimentally evaluate nucleation kinetics and empirically correlate column backmixing characteristics. Calculations based on stage solids mass balances showed that the mass concentration parameter, θ, did not exceed 0.1 for any of the column crystallizer runs. More detailed descriptions of the apparatus and experimental results will be included in a subsequent paper.

Examples of the steady state gypsum product CSD's from pure countercurrent multistage and single-stage crystallizer experiments are shown in Figure 9. For CSD analysis a 128-channel particle size analyzer, (Model 80XY, Particle Data Inc.) fitted with a 300 μm orifice tube, was used. To simplify the figure the data points shown are averaged over eight adjacent channels. Clearly, the four-stage CCSF crystallizer yields an enlarged product CSD compared to the MSMPR base case.

However, when this size improvement is evaluated using numerically calculated CSD moments (Randolph and Larson, 1971), the ratio $\bar{L}_4/\bar{L}_{MSMPR}$ has a value of 1.11. This result is to be expected, in light of the gypsum nucleation kinetics shown (point A) in Figure 8. The physical reason for this is that primary and secondary nucleation sources are comparable in strength for gypsum crystallization. Other investigators (White and Hoa, 1977; Etherton and Randolph, 1981) have also obtained kinetic parameters that lie close to the plotted breakeven boundaries.

For this application an alternative feed/product arrangement that would introduce feed solute to a stage of relatively lower solids concentration should be favorable.

Conclusion

A new staged crystallizer concept and corresponding population balance model have been described. Analysis based on this model for a simplified single-feed case shows that a pure countercurrent operating mode yields product size enlargement if secondary nucleation is comparatively unimportant. Should secondary sources of nuclei be significant the column design may

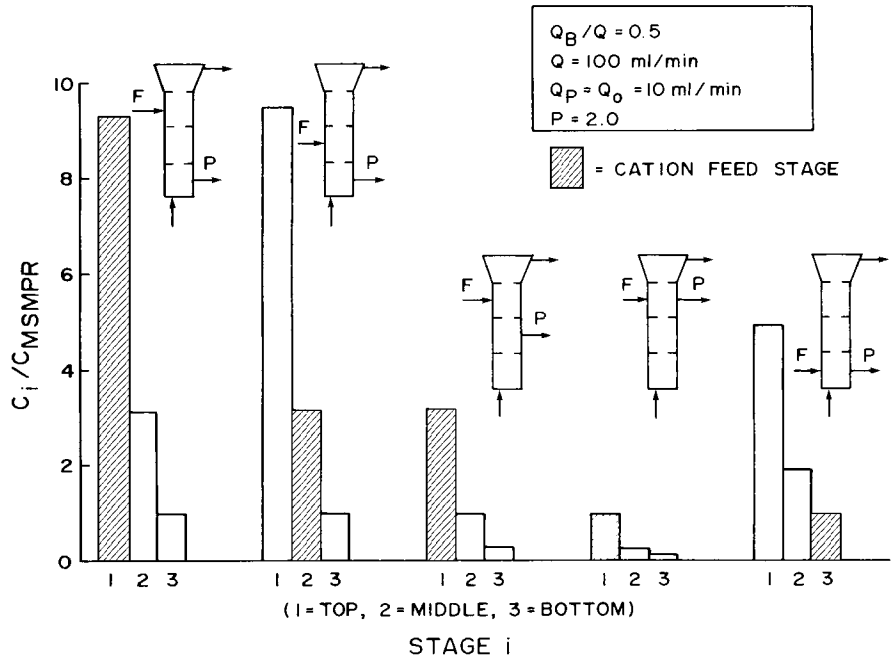

Figure 7. Effect of feed/product arrangement on solids concentration profile for three-stage crystallizer example.

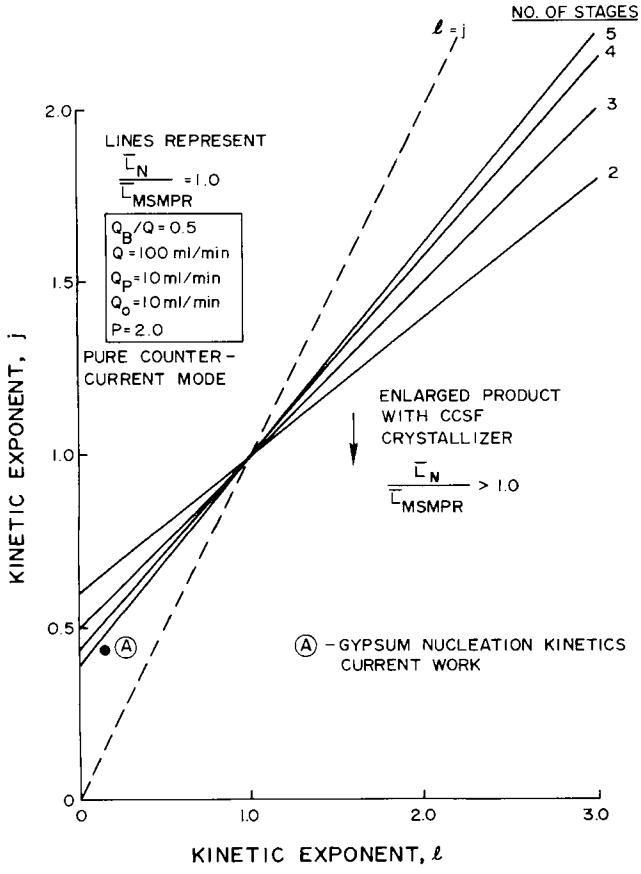

Figure 8. Nucleation kinetic regimes yielding improved product size for pure countercurrent staged crystallizers having two to five stages.

favor fewer stages, or a feed/product stream configuration resulting in lower solids concentration in the feed stage. The main physical factor that leads to product enlargement is increased holdup of solids, providing additional crystal surface area that results in suppressed primary nucleation.

Because of its inherent design and operating flexibility, the CCSF crystallizer may be used in a wide variety of applications. It has been demonstrated that staged crystallizer hydrodynamics permit the solids concentration profile to be controlled. Depending on the kinetic relationship between solids concentration and nucleation rate, it may be favorable to introduce feed to a stage of relatively high or low concentration. The ability to specify a solute feed profile so as to optimally control stage growth rates offers the potential for product size enlargement in systems that may be limited by primary nucleation. Since intrinsic nucleation kinetics vary greatly, a method of evaluating staged crystallizer designs for size improvement, based on kinetic parameter values, has been developed.

Acknowledgment

The authors would like to acknowledge the financial assistance of NSF Grant No. CPE-8211671-01 in support of this work.

Notation

$[A]$ = anion concentration, mol/L
$[A_{N+1}]$ = anion concentration in feed stream, mol/L
B = tridiagonal coefficient matrix
B^o = nuclei birth rate, no/mL · s
C = solids mass concentration, g/mL
f = anion feed fraction
F = cation feed stream
g = cation feed fraction
G = crystal growth rate, μm/s
i = stage index
j = nucleation kinetic exponent
k = order of CSD moment
ℓ = nucleation kinetic exponent
L = characteristic crystal dimension, μm

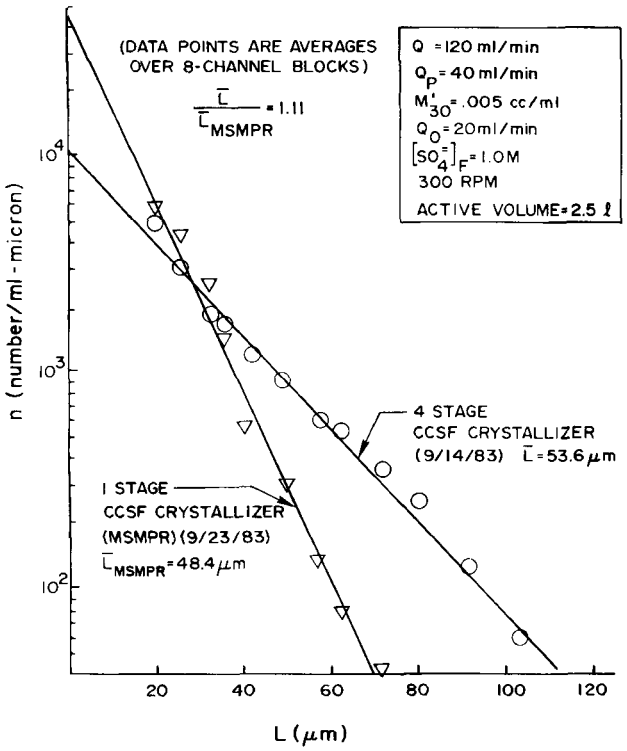

Figure 9. Comparison of experimental gypsum product CSD obtained from four-stage CCSF crystallizer and equivalent MSMPR unit.

$\bar{L}$ = (m_3/m_2) volume average particle size, μm
L_c = critical particle diameter for washout in overflow stream
m_k = kth order moment of CSD
$m'_{3,0}$ = cation feed concentration, cm^3/mL, (slurry form)
n = crystal population density function, no./mL · μ
n^o = nuclei population density parameter, no./mL · μ
N = total number of stages
P = mass concentration factor of product withdrawal port, product stream
Q = cation feed flow rate, bulk upflow rate, mL/min
Q_o = cation feed flow rate, mL/min
Q_p = product flow rate, mL/min
Q_B = interstage backmixing flow rate, mL/min
S = unit step function
V = volume
V_T = total active crystallizer volume
x = dimensionless coefficient, Table 1
y = dimensionless coefficient, Table 1
z = dimensionless coefficient, Table 1

Greek letters

β_N = flow factor coefficient for N-stage crystallizer
γ = particle volume factor
Γ = fractional moment of material in overflow stream
κ_n = prefactor in nucleation model
ρ_s = molar solids density of product, mol/cm^3
ρ'_s = molar density of cation feed material, mol/cm^3 (for slurry feed)
θ = interstage mass concentration parameter
τ = residence time, s

Subscripts

b = bottom stage feed
i = stage index
k = moment index
m = middle stage feed
MSMPR = single stage base case
N = column bottom stage, total number of stages
p = product stage
o = zeroth stage, clarifier

Literature Cited

Beckman, J. R., and R. W. Farmer, "Improved CSD by a Countercurrent Tower Crystallizer," Paper No. 56d, AIChE Meet., Atlanta (Mar., 1984).

Betts, W. D., and G. W. Girling, "Continuous Column Crystallization," *Progress in Separation and Purification*, E. S. Perry and C. J. Van Oss, eds., Wiley-Interscience, New York, **4** (1971).

Chien, Henry H. Y., "Simulation of a Countercurrent Equilibrium Crystallizer," *IEC Proc. Des. Dev.*, **23**, 279 (1984).

Desai, R. M., et al., "Collision Breeding: A Function of Crystal Moments and Degree of Mixing," *AIChE J.*, **20**, 43 (1974).

Devyatykh, G. G., et al., "Effect of Longitudinal Mixing on the Extent of Purification of Materials by the Method of Countercurrent Crystallization from a Melt," *Teor. Osnovy Khim. Teckhnol.* (Engl. trans.), **11**, 263 (1977).

Etherton, D. L., and A. D. Randolph, "Nucleation/Growth Rate Kinetics of Gypsum in Simulated FGD Liquors: Some Process Configurations for Increasing Particle Size," *AIChE Symp. Ser. No. 211*, **77**, 87 (1981).

Henry, J. D., and J. E. Powers, "Experimental and Theoretical Investigation of Continuous-Flow Column Crystallization," *AIChE J.*, **16**, 1,055 (1970).

Larson, M. A., and P. R. Wolff, "Crystal Size Distributions from Multistage Crystallizers," *AIChE Symp. Ser. No. 110*, **67**, 97 (1971).

Matz, G., "Modern Trends in Technical Crystallization," *J. Cryst. Growth*, **48**, 563 (1980).

Mullin, J. W., "Bulk Crystallization," *Crystal Growth*, B. R. Pamplin, ed., Pergamon, Oxford, England (1980).

Player, M. R., "Mathematical Analysis of Column Crystallization," *IEC Proc. Des. Dev.*, **8**, 210 (1969).

Randolph, A. D., and M. A. Larson, "Transient and Steady State Size Distributions in Continuous Mixed Suspensions Crystallizers," *AIChE J.*, **8**, 639 (1962).

———, *Theory of Particulate Processes*, Academic Press, New York (1971).

Randolph, A. D., and C. S. Tan, "Numerical Design Techniques for Staged Classified Recycle Crystallizers: Examples of Continuous Alumina and Sucrose Crystallizers," *IEC Proc. Des. Dev.*, **17**, 189 (1978).

Takegami, N., et al., "Industrial Molten Fractional Crystallization," *Industrial Crystallization 84*, S. J. Jancic and E. J. deJong, eds., Elsevier, Amsterdam (1984).

White, E. T., and L. T. Hoa, "Mass Transfer Studies in Particulate Systems Using the Population Balance Approach—The Growth of Gypsum Crystals," *2nd Australasian Conf. Heat Mass Transfer*, Sydney (1977).

Youngquist, G. R., and A. D. Randolph, "Secondary Nucleation in a Class II System: Ammonium Sulfate-Water," *AIChE J.*, **18**, 421 (1972).

Zwietering, T. N., "Suspending of Solid Particles in Liquid by Agitators," *Chem. Eng. Sci.*, **8**, 144 (1958).

Manuscript received Jan. 11, and revision received Oct. 3, 1985.